J. Fluid Mech. (1993), *vol.* 250, *pp.* 143–167

Microstructure suspended in three-dimensional flows

By ANDREW J. SZERI[1] AND L. GARY LEAL[2]

[1] Department of Mechanical and Aerospace Engineering, University of California, Irvine, CA 92717-3975, USA

[2] Department of Chemical and Nuclear Engineering, University of California, Santa Barbara, CA 93106, USA

(Received 17 April 1992 and in revised form 29 October 1992)

The dynamical behaviour of stretchable, orientable microstructure suspended in a general three-dimensional fluid flow is investigated. Model equations given by Olbricht, Rallison & Leal (1982) are examined in the case of microstructure travelling through arbitrarily complicated flows of the carrier fluid. As in the two-dimensional analysis of Szeri, Wiggins & Leal (1991), one must first treat the orientation dynamics problem; only then can the equation for stretch of the microstructure be analyzed rationally. In three-dimensional flows that are steady in the Lagrangian frame, attractors for the orientation dynamics are shown to be equilibria or limit cycles; this asymptotic behaviour was first deduced by Bretherton (1962). In three-dimensional flows that are time periodic in the Lagrangian frame (e.g. recirculating flows), the orientation dynamics may be characterized by periodic or quasi-periodic attractors. Thus, robust (generic) behaviour in these cases is always characterized by a single global attractor; there is no asymptotic dependence of orientation dynamics on the initial orientation. The type of asymptotic orientation dynamics – steady, periodic, or quasi-periodic – is signified by a simple criterion. Details of the relevant bifurcations, as well as history-dependent strong flow criteria are developed. Examples which illustrate the various types of behaviour are given.

1. Introduction

The dynamical behaviour of particles, droplets or polymer molecules in suspension (collectively referred to as microstructure) is an important subject in a number of different fields. A particularly interesting aspect is the interaction of the flow with the suspended phase. In sufficiently dilute suspensions, the influence of the microstructure on the flow is very small; thus the interaction problem is decoupled in the case of infinite dilution. In this context, it is of interest to establish, in as general a framework as possible, the dynamical behaviour that may occur for microstructure suspended in flow fields of known form.

Many authors, as reviewed by Szeri, Wiggins & Leal (1991), have examined this question in the light of a further simplification, namely, that the known flow field is steady and spatially homogeneous. While the assumption that the effect of the microstructure on the flow is minimal is valid in the limit of infinite dilution of the suspended phase, the assumption of a steady and spatially homogeneous flow field yields dynamical behaviour that is not general.

In Szeri, Wiggins & Leal (1991, hereinafter referred to as SWL), the means of analysing the dynamics of suspended microstructure in complicated two-dimensional

flows were developed. The key idea is that the dynamics of the suspended phase differ in *simple* flows (*steady* from the point of view of the moving particle) and *complex* flows (*unsteady* from the point of view of the particle) because the forcing of the conformation evolution equations is autonomous or non-autonomous, respectively. Thus in complex flow, it makes sense to analyse conformation evolution equations only over an interval of time, i.e. one must take history into account. The primary results of that analysis are: (i) a necessary and sufficient condition for stretching of microstructure (i.e. a 'strong flow criterion') in complex, two-dimensional flows that takes history into account; and (ii) conditions for the existence of *time-dependent attracting orientations* of microstructure in complex flows, that are analogous to steady, equilibrium orientations for microstructure in simple flows. These time-dependent attracting orientations were later observed in experiments reported by Szeri, Milliken & Leal (1992). In this paper, our goal is to extend the analysis to three-dimensional flows.

We begin the analysis in §2 by listing the governing equations and discussing the method of solution of the orientation and stretch dynamics problems for a particle in a general flow field. Section 3 involves a characterization of the orientation dynamics and stretch of particles suspended in a (known) three-dimensional flow field that is steady in the Lagrangian frame. Typical orientation dynamics is characterized by either a single attracting orientation to which all particles tend asymptotically (as $t \to \infty$), or a limit cycle of orientations to which all particles tend asymptotically. A strong flow criterion is derived. In §4, we treat orientation and stretch dynamics of particles that are forced by a flow field that is periodic in the Lagrangian frame. This situation is important for particles in recirculating flows that are steady in the Eulerian frame, for example. The difference from the analysis of §3 is that the history of flows experienced by the particles is non-trivial. We find that either particles tend asymptotically to a limit cycle of orientations with the same period as the flow, or particles tend asymptotically to a quasi-periodic attractor. We develop strong flow criteria, where possible, and consider in detail an example problem.

In §§5 and 6, our goal is to shed light on the stretching behaviour in the absence of full information about the flow or the orientation dynamics. In §5, we derive a general history-dependent strong flow criterion that applies to microstructure in a general time-dependent flow over a time interval $0 < t < T$. In §6, we derive simple weak flow criteria that apply along a given particle path, or over a region of the flow. Finally in §7, we give our conclusions.

2. Dynamical equations and solutions

We consider the dynamical behaviour of a particle, suspended in a flow, which is small with respect to lengthscales of the flow, and described by a single axial (state) vector. Olbricht, Rallison & Leal (1982) demonstrate that the microdynamical equations for a number of different physical systems may be collapsed onto a single equation depending on various parameters. Physically, the behaviour of the particle evolves according to a locally linear flow field. The model evolution equation for the state vector $\boldsymbol{R}$ of an element of the suspended phase is

$$\frac{\mathrm{d}}{\mathrm{d}t}\boldsymbol{R} = \boldsymbol{\Omega}\cdot\boldsymbol{R} + G\left[\boldsymbol{E}\cdot\boldsymbol{R} - \frac{F}{F+1}\frac{\boldsymbol{R}\cdot\boldsymbol{E}\cdot\boldsymbol{R}}{|\boldsymbol{R}|^2}\boldsymbol{R}\right] - \frac{\alpha}{F+1}\boldsymbol{R}. \tag{2.1}$$

In (2.1), $\boldsymbol{\Omega}$ and $\boldsymbol{E}$ are the local vorticity and rate-of-strain tensors, respectively, and the parameters $0 \leqslant G \leqslant 1$, $\alpha \geqslant 0$ and $F \geqslant 0$ correspond to the shape factor, the elastic

modulus and the internal viscosity of the microstructure, respectively. Note that $G = 1$, $\alpha = F = 0$ yields an equation for microstructure that rotates and stretches exactly as an infinitesimal line element of the fluid. We assume that the microstructure follows the same paths as fluid particles. This assumption may be too restrictive for heavier particles.

It will be convenient in our analysis to separate the stretch and orientation degrees of freedom; thus we define $\boldsymbol{R} = \rho \boldsymbol{u}$, where $\boldsymbol{R} \cdot \boldsymbol{R} = \rho^2$ and $\boldsymbol{u} \cdot \boldsymbol{u} = 1$, following Olbricht *et al.* (1982). This leads to separate evolution equations for the length of the microstructure ρ and the orientation $\boldsymbol{u}$:

$$\frac{\mathrm{d}}{\mathrm{d}t}\boldsymbol{u} = (\boldsymbol{\Omega}(t) + G\boldsymbol{E}(t)) \cdot \boldsymbol{u} - G\boldsymbol{E}(t) : \boldsymbol{uuu}$$

$$= \boldsymbol{\kappa}(t) \cdot \boldsymbol{u} - \boldsymbol{\kappa}(t) : \boldsymbol{uuu}, \quad \boldsymbol{\kappa}(t) = \boldsymbol{\Omega}(t) + G\boldsymbol{E}(t), \tag{2.2a}$$

$$\frac{1}{\rho}\frac{\mathrm{d}}{\mathrm{d}t}\rho = \frac{G}{F+1}\boldsymbol{E}(t) : \boldsymbol{uu} - \frac{\alpha}{F+1}. \tag{2.2b}$$

Clearly, one can obtain ρ after solving (2.2*a*) for the orientation $\boldsymbol{u}(t; \boldsymbol{u}_0)$, which depends on the initial orientation $\boldsymbol{u}_0$; this procedure yields $\rho(t; \rho_0, \boldsymbol{u}_0)$.

The solution of the orientation evolution equation may be obtained via the equivalent deformation gradient tensor approach; see Bretherton (1962) and also Lipscomb *et al.* (1988). We define the equivalent deformation gradient tensor $\boldsymbol{Q}$ to be the solution of the linear equation

$$\frac{\mathrm{d}}{\mathrm{d}t}\boldsymbol{Q} = \boldsymbol{\kappa}(t) \cdot \boldsymbol{Q}, \quad \boldsymbol{Q}(0) = \boldsymbol{I}, \tag{2.3}$$

where $\boldsymbol{I}$ is the identity tensor. Then the solution of (2.2*a*) may be written

$$\boldsymbol{u}(t; \boldsymbol{u}_0) = \frac{\boldsymbol{Q}(t) \cdot \boldsymbol{u}_0}{|\boldsymbol{Q}(t) \cdot \boldsymbol{u}_0|}. \tag{2.4}$$

This procedure works whether $\boldsymbol{\kappa}$ depends on time (*complex* flow) or not (*simple* flow). Of course, the solution of the nine coupled equations (2.3) may be difficult when these are equations with time-dependent coefficients. Physically, the equivalent deformation gradient tensor $\boldsymbol{Q}(t)$ corresponds to the true deformation gradient tensor between reference ($t = 0$) and current (t) configurations in physical space, when the shape factor G is equal to unity. For a given initial orientation $\boldsymbol{u}_0$, it is a simple matter to integrate the stretch equation (2.2*b*) and obtain

$$\frac{\rho(T)}{\rho_0} = \exp\left[\frac{1}{F+1}\left(G\int_0^T \boldsymbol{E}(t) : \boldsymbol{uu}(t; \boldsymbol{u}_0)\,\mathrm{d}t - \alpha T\right)\right]. \tag{2.5}$$

Much of the analysis that follows depends on the eigenvalues of the tensors $\boldsymbol{\kappa}$ and $\boldsymbol{Q}$. There are two important properties of these tensors that we shall make frequent use of: (i) $\mathrm{tr}[\boldsymbol{\kappa}(t)] = 0$, due to incompressibility, and (ii) $\det[\boldsymbol{Q}(t)] = 1$, due to incompressibility and to equation (2.3). The latter property is proved as follows. We make use of a Taylor series and equation (2.3) to write

$$\boldsymbol{Q}(t + \Delta t) = \boldsymbol{Q}(t) + \Delta t\, \boldsymbol{\kappa}(t) \cdot \boldsymbol{Q}(t) + o(\Delta t).$$

The determinant of $\boldsymbol{Q}(t + \Delta t)$ is

$$\det[\boldsymbol{Q}(t + \Delta t)] = \det[\boldsymbol{I} + \Delta t \boldsymbol{\kappa}(t)] \det[\boldsymbol{Q}(t)] + o(\Delta t).$$

The first determinant on the right-hand side is computed using the characteristic polynomial, which gives

$$\det[\boldsymbol{I}+\Delta t\boldsymbol{\kappa}(t)] = 1+(\Delta t)\,\mathrm{tr}[\boldsymbol{\kappa}(t)]+o(\Delta t).$$

Thus, the time derivative of $\det[\boldsymbol{Q}(t)]$ may be written

$$(\mathrm{d}/\mathrm{d}t)\det[\boldsymbol{Q}(t)] = \mathrm{tr}[\boldsymbol{\kappa}(t)]\det[\boldsymbol{Q}(t)].$$

This quantity is zero, owing to incompressibility of the fluid. Hence, the equivalent deformation gradient tensor retains its initial determinant for all time, which is one.

We remind the reader that the true deformation gradient tensor ($\boldsymbol{Q}$ when $G = 1$) associated with motion of a continuum has a determinant of unity if and only if the continuum is incompressible. The previous analysis shows that the property $\det[\boldsymbol{Q}(t)] = 1$ also holds for $G \neq 1$.

3. Simple flows

When the flow is simple ($\boldsymbol{\kappa}(t) =$ constant), then the right-hand-side of (2.2*a*) is a steady vector field on the sphere of orientations. In this section, we argue from topological considerations and from knowledge of the form of the form of the solution (2.4), that there are two generic (i.e. 'typical') types of dynamical behaviour in simple three-dimensional flows. Either particles are eventually attracted to a single equilibrium orientation, or particles are eventually attracted to a limit cycle of orientations that lies in a planar subset of the sphere of orientations. The asymptotic behaviour we describe here was deduced by Bretherton (1962). In this section we review these results in a modern setting, and explore the relevant bifurcations that connect the two types of generic behaviour that may occur.

3.1. *Orientation dynamics*

From (2.4), an equilibrium orientation $\boldsymbol{U}_e$ satisfies

$$\boldsymbol{U}_e = \frac{\boldsymbol{Q}(t)\cdot\boldsymbol{U}_e}{|\boldsymbol{Q}(t)\cdot\boldsymbol{U}_e|}. \tag{3.1}$$

In other words, an equilibrium orientation must be a (steady) eigenvector of the equivalent deformation gradient tensor $\boldsymbol{Q}(t)$, with the associated eigenvalue $|\boldsymbol{Q}(t)\cdot\boldsymbol{U}_e|$. It is clear from (2.2*a*) that an equilibrium orientation $\boldsymbol{U}_e$ is also an eigenvector of the constant tensor $\boldsymbol{\kappa}$:

$$\boldsymbol{\kappa}\cdot\boldsymbol{U}_e = (\boldsymbol{\kappa}\colon\boldsymbol{U}_e\,\boldsymbol{U}_e)\,\boldsymbol{U}_e. \tag{3.2}$$

Thus, the eigenvalue of $\boldsymbol{\kappa}$ associated with the eigenvector $\boldsymbol{U}_e$ is $\boldsymbol{\kappa}\colon\boldsymbol{U}_e\,\boldsymbol{U}_e$.

In order to establish the relationship between the two eigenvalues $\boldsymbol{\kappa}\colon\boldsymbol{U}_e\,\boldsymbol{U}_e$ and $|\boldsymbol{Q}(t)\cdot\boldsymbol{U}_e|$ corresponding to the eigenvector $\boldsymbol{U}_e$, we take the inner product of (2.3) with an equilibrium orientation $\boldsymbol{U}_e$ and make use of (3.1) and (3.2) to obtain

$$(\mathrm{d}/\mathrm{d}t)\,\boldsymbol{Q}\cdot\boldsymbol{U}_e = |\boldsymbol{Q}(t)\cdot\boldsymbol{U}_e|\,(\boldsymbol{\kappa}\colon\boldsymbol{U}_e\,\boldsymbol{U}_e)\,\boldsymbol{U}_e. \tag{3.3}$$

Now we consider the evolution of the eigenvalue $|\boldsymbol{Q}(t)\cdot\boldsymbol{U}_e|$. Differentiation with respect to time, and use of (3.3) yields

$$(\mathrm{d}/\mathrm{d}t)\,|\boldsymbol{Q}(t)\cdot\boldsymbol{U}_e| = |\boldsymbol{Q}(t)\cdot\boldsymbol{U}_e|\,(\boldsymbol{\kappa}\colon\boldsymbol{U}_e\,\boldsymbol{U}_e),$$

with solution

$$|\boldsymbol{Q}(t)\cdot\boldsymbol{U}_e| = \exp(t\boldsymbol{\kappa}\colon\boldsymbol{U}_e\,\boldsymbol{U}_e). \tag{3.4}$$

Thus, the eigenvalue of the equivalent deformation gradient tensor $\boldsymbol{Q}(t)$, $|\boldsymbol{Q}(t)\cdot U_e|$, is the exponential of the associated eigenvalue of $\boldsymbol{\kappa}$, $\boldsymbol{\kappa}: U_e U_e$, multiplied by time.

The range of possible dynamics in simple three-dimensional flows is thus limited by the properties of *generic* 3×3, steady, traceless tensors $\boldsymbol{\kappa}$. One can classify generic tensors $\boldsymbol{\kappa}$ based on their eigenvalues: either $\boldsymbol{\kappa}$ has one real and two complex-conjugate eigenvalues, or it has three real, distinct eigenvalues. Non-generic tensors $\boldsymbol{\kappa}$ have an eigenvalue with zero real part, or two or more equal eigenvalues. A slight perturbation of a non-generic tensor $\boldsymbol{\kappa}$ changes it into a generic tensor. Hence the commonly analysed flows: simple shear (eigenvalue with zero real part), and bi-axial or uniaxial flow (two eigenvalues equal) are not generic. We analyse the two generic cases in turn.

Case 1: $\boldsymbol{\kappa}$ has three distinct, real, non-zero eigenvalues

When $\boldsymbol{\kappa}$ has three real, distinct eigenvalues (λ_1, λ_2 and λ_3), Schur's theorem (Cullen 1979) asserts that there are orthogonal coordinates in which the tensor $\boldsymbol{\kappa}$ takes the form

$$\boldsymbol{\kappa}=\begin{bmatrix}\lambda_1 & \kappa_{12} & \kappa_{13}\\ 0 & \lambda_2 & \kappa_{23}\\ 0 & 0 & \lambda_3\end{bmatrix}. \tag{3.5}$$

Incompressibility requires $\lambda_1+\lambda_2+\lambda_3=0$. Equation (2.3) may be solved to obtain

$$\boldsymbol{Q}(t)=\begin{bmatrix}\exp[t\lambda_1] & Q_{12}(t) & Q_{13}(t)\\ 0 & \exp[t\lambda_2] & Q_{23}(t)\\ 0 & 0 & \exp[t\lambda_3]\end{bmatrix}, \tag{3.6}$$

where

$$Q_{12}(t)=\frac{e^{(\lambda_1-\lambda_2)t}\kappa_{12}}{\lambda_1-\lambda_2},\quad Q_{23}(t)=\frac{e^{(\lambda_2-\lambda_3)t}\kappa_{23}}{\lambda_2-\lambda_3},$$

$$Q_{13}(t)=\frac{1}{(\lambda_1-\lambda_2)(\lambda_1-\lambda_3)(\lambda_2-\lambda_3)}[e^{\lambda_1 t}(\lambda_2-\lambda_3)(\kappa_{12}\kappa_{23}+\kappa_{13}(\lambda_1-\lambda_2))$$
$$+e^{\lambda_2 t}(\lambda_3-\lambda_1)\kappa_{12}\kappa_{23}+e^{\lambda_3 t}(\lambda_1-\lambda_2)(\kappa_{12}\kappa_{23}-\kappa_{13}(\lambda_2-\lambda_3))].$$

The associated particle orientation dynamics may be understood from (2.4). One can show that there are three invariant great circles of the sphere of orientations, i.e. three circles, centred at the origin of the sphere of orientations associated with a given particle, on which the motion is invariant. The invariant great circles lie in planes normal to the vectors

$$\boldsymbol{n}^{(1)}=\begin{pmatrix}(\lambda_1-\lambda_2)(\lambda_1-\lambda_3)\\ \kappa_{12}(\lambda_1-\lambda_3)\\ \kappa_{12}\kappa_{23}+\kappa_{13}(\lambda_1-\lambda_2)\end{pmatrix},\quad \boldsymbol{n}^{(2)}=\begin{pmatrix}0\\ \lambda_2-\lambda_3\\ \kappa_{23}\end{pmatrix},\quad \boldsymbol{n}^{(3)}=\begin{pmatrix}0\\ 0\\ 1\end{pmatrix}. \tag{3.7}$$

Hence $\boldsymbol{u}\cdot\boldsymbol{n}^{(i)}=0$ implies $\boldsymbol{n}^{(i)}\cdot \mathrm{d}\boldsymbol{u}/\mathrm{d}t=0$; in fact these relations determine the normals to the three invariant great circles. The three invariant great circles provide a framework for understanding the orientation dynamics of all initial orientations. The equilibrium orientations corresponding to λ_i are at the *intersections* of the great circles lying in the planes normal to $\boldsymbol{n}^{(i)}$; hence,

$$U_e^{(1)}=\pm\begin{pmatrix}1\\0\\0\end{pmatrix},\quad U_e^{(2)}=\pm\begin{pmatrix}-\kappa_{12}\\ \lambda_1-\lambda_2\\ 0\end{pmatrix},\quad U_e^{(3)}=\pm\begin{pmatrix}\kappa_{12}\kappa_{23}+\kappa_{13}(\lambda_3-\lambda_2)\\ \kappa_{23}(\lambda_3-\lambda_1)\\ (\lambda_3-\lambda_1)(\lambda_3-\lambda_2)\end{pmatrix}. \tag{3.8}$$

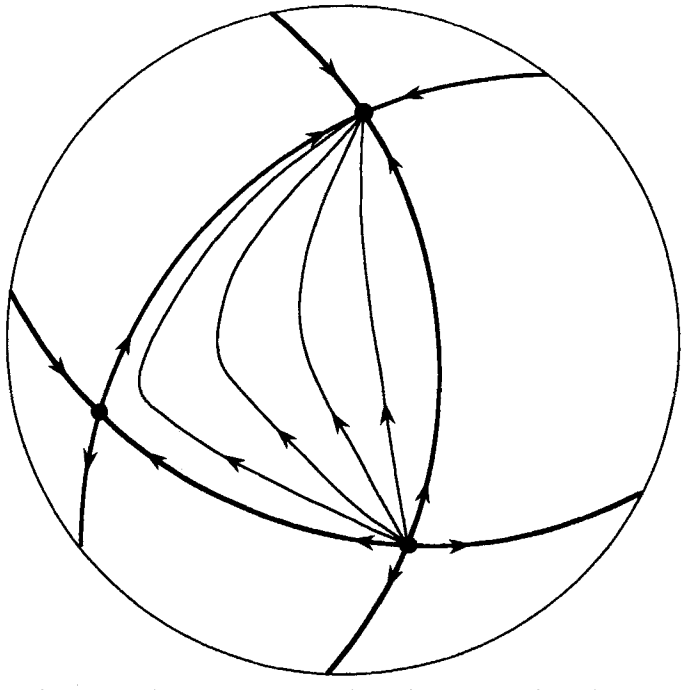

FIGURE 1. A sketch of the phase portrait in orientation space when the equivalent deformation gradient tensor has three real, distinct eigenvalues. The heavy curves are the invariant great circles. At the intersection of the invariant great circles are the equilibrium orientations.

The three equilibrium orientations (3.8) correspond to six fixed points of the vector field on the surface of the unit sphere, owing to the symmetry $\boldsymbol{u} \to -\boldsymbol{u}$. A sketch of orientation space is shown in figure 1. Note that the three equilibrium orientations given in (3.8) are not normalized, as the formulae are too long. The stability types of the six fixed points on the surface of the sphere are constrained, as shown in Arnol'd (1973). In our case, these restrictions imply that there must be two nodes (or foci) and one saddle point in any hemisphere, among the six fixed points we know to exist. Any of the three invariant great circles serves to divide the sphere of orientations into two hemispheres. Each hemisphere is further divided into four cells, where each boundary of each cell is an arc of one of the invariant great circles. The cells are therefore spherical triangles, with equilibrium orientations at the vertices. Because one of the vertices must be a saddle point, and the other two nodes, the nodes must be of differing stability type, as indicated in the sketch.

One can analyse the stability of equilibrium orientations by a linear stability analysis of (2.2a). We let $\boldsymbol{u}(t:\boldsymbol{u}_0) = \boldsymbol{U}_{\mathrm{e}}^{(i)} + \delta\boldsymbol{u}(t)$, where $\delta\boldsymbol{u}(t)$ is a perturbation. Equation (2.2a) may be written

$$(\mathrm{d}/\mathrm{d}t)\,\delta\boldsymbol{u} = \boldsymbol{M}\cdot\delta\boldsymbol{u} + o(|\delta\boldsymbol{u}|)$$

where

$$\boldsymbol{M} = \boldsymbol{\kappa} - (\boldsymbol{GE}:\boldsymbol{U}_{\mathrm{e}}^{(i)}\,\boldsymbol{U}_{\mathrm{e}}^{(i)})[\boldsymbol{I} + 2\boldsymbol{U}_{\mathrm{e}}^{(i)} \otimes \boldsymbol{U}_{\mathrm{e}}^{(i)}] + 2\boldsymbol{U}_{\mathrm{e}}^{(i)} \otimes (\boldsymbol{\Omega}\cdot\boldsymbol{U}_{\mathrm{e}}^{(i)}).$$

The norm of the perturbation $|\delta\boldsymbol{u}(t)|$ evolves according to

$$\begin{aligned}\tfrac{1}{2}(\mathrm{d}/\mathrm{d}t)\,|\delta\boldsymbol{u}|^2 &= \delta\boldsymbol{u}\cdot\boldsymbol{M}\cdot\delta\boldsymbol{u} + o(|\delta\boldsymbol{u}|^2)\\ &= \left[\frac{\delta\boldsymbol{u}}{|\delta\boldsymbol{u}|}\cdot\boldsymbol{GE}\cdot\frac{\delta\boldsymbol{u}}{|\delta\boldsymbol{u}|} - \boldsymbol{U}_{\mathrm{e}}^{(i)}\cdot\boldsymbol{GE}\cdot\boldsymbol{U}_{\mathrm{e}}^{(i)}\right]|\delta\boldsymbol{u}|^2 + o(|\delta\boldsymbol{u}|^2).\end{aligned}$$

In the coordinate system in which $\boldsymbol{\kappa}$ has the representation (3.5), this equation reads

$$\frac{1}{2}\frac{\mathrm{d}}{\mathrm{d}t}|\delta\boldsymbol{u}|^2 = [\delta\boldsymbol{u}]^{\mathrm{T}}\begin{bmatrix}\lambda_1-\lambda_{(i)} & \kappa_{12} & \kappa_{13}\\ 0 & \lambda_2-\lambda_{(i)} & \kappa_{23}\\ 0 & 0 & \lambda_3-\lambda_{(i)}\end{bmatrix}[\delta\boldsymbol{u}]+o(|\delta\boldsymbol{u}|^2).$$

Now, if we take $i=1$, then $\boldsymbol{U}_{\mathrm{e}}^{(i)}=(1,0,0)$ and $\delta\boldsymbol{u}=(0,\delta u_2,\delta u_3)$ by virtue of the fact that $\delta\boldsymbol{u}\cdot\boldsymbol{U}_{\mathrm{e}}^{(i)}=0$. Thus we have

$$\frac{1}{2}\frac{\mathrm{d}}{\mathrm{d}t}|\delta\boldsymbol{u}|^2 = (\delta u_2\,\delta u_3)\begin{bmatrix}\lambda_2-\lambda_1 & \kappa_{23}\\ 0 & \lambda_3-\lambda_1\end{bmatrix}\begin{pmatrix}\delta u_2\\ \delta u_3\end{pmatrix}+o(|\delta\boldsymbol{u}|^2).$$

As one might expect, if $\lambda_1>\lambda_2>\lambda_3$, then the quadratic form is negative definite and so the equilibrium is stable. Hence, the equilibrium orientation (eigenvector of $\boldsymbol{\kappa}$) which corresponds to the maximum eigenvalue of $\boldsymbol{\kappa}$ is the stable one. The asymptotic behaviour of microstructure in simple flows where $\boldsymbol{\kappa}$ has three real, distinct eigenvalues is as follows. The cell boundaries are boundaries of the orbits. Within each cell, orbits tend to the unstable node as $t\to-\infty$, and to the stable node as $t\to+\infty$. This family of orbits limits on the saddle point, as shown in figure 1.

As a special case of the preceding analysis, one may consider irrotational flow ($\boldsymbol{\Omega}=0$). In this case $\boldsymbol{\kappa}$ may be written as a diagonal tensor by an orthogonal change of coordinates. Then the invariant great circles lie on planes normal to the vectors $\boldsymbol{n}^{(i)}=\boldsymbol{e}_i$ parallel to the orthogonal basis. The equilibrium orientations are then coincident with the normal vectors of the invariant planes, i.e. $\boldsymbol{U}_{\mathrm{e}}^{(i)}=\pm\boldsymbol{n}^{(i)}$. Finally, the equivalent deformation gradient tensor has the special form $Q_{ij}=0\,(i\neq j)$ and $Q_{ii}=\exp[t\lambda_i]$. In this situation, it is readily seen that the microstructure lines up with the eigenvector of the rate-of-strain tensor associated with the maximum eigenvalue.

Case 2: $\boldsymbol{\kappa}$ has 1 real, non-zero eigenvalue, and a complex-conjugate pair

In case 2, there is but one equilibrium orientation $\boldsymbol{U}_{\mathrm{e}}$, with corresponding eigenvalue $\lambda_1\neq 0$. By Schur's theorem, there is an orthogonal change of coordinates in which the tensor $\boldsymbol{\kappa}$ takes the form

$$\boldsymbol{\kappa}=\begin{bmatrix}\lambda_1 & \kappa_{12} & \kappa_{13}\\ 0 & \kappa_{22} & \kappa_{23}\\ 0 & \kappa_{32} & \kappa_{33}\end{bmatrix}. \tag{3.9}$$

Corresponding to the fact that the other eigenvalues of $\boldsymbol{\kappa}$ are assumed to be a complex-conjugate pair, we must have

$$4\kappa_{23}\kappa_{32}<-(\kappa_{22}-\kappa_{33})^2.$$

Equation (2.3) has the solution

$$\boldsymbol{Q}(t)=\begin{bmatrix}\exp(t\lambda_1) & Q_{12}(t) & Q_{13}(t)\\ 0 & Q_{22}(t) & Q_{23}(t)\\ 0 & Q_{32}(t) & Q_{33}(t)\end{bmatrix}.$$

The formulae for $Q_{ij}(t)$ can be computed without difficult, but are too long to be included here.

In case 2, there is a single invariant great circle, which lies in the plane normal to the vector

$$\boldsymbol{n}=\begin{pmatrix}(\lambda_1-\kappa_{22})(\lambda_1-\kappa_{33})-\kappa_{23}\kappa_{32}\\ \kappa_{12}(\lambda_1-\kappa_{33})+\kappa_{13}\kappa_{32}\\ \kappa_{13}(\lambda_1-\kappa_{22})+\kappa_{12}\kappa_{23}\end{pmatrix}. \tag{3.10}$$

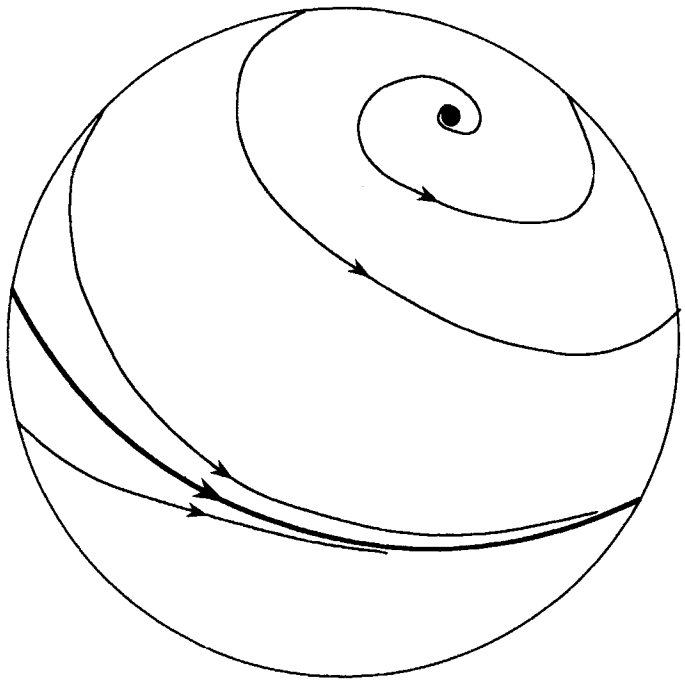

FIGURE 2. Phase portrait of the sphere of orientations when the equivalent deformation gradient tensor has but one real eigenvalue. Note the invariant great circle, which is a stable limit cycle when the equilibrium orientation is unstable, and unstable limit cycle when the equilibrium orientation is stable (arrows reversed).

The equilibrium orientation in these coordinates is $\boldsymbol{U}_e = \pm(1,0,0)$. As $\boldsymbol{U}_e$ is not contained in the great circle, the circle constitutes a periodic solution.

The stability of $\boldsymbol{U}_e$ may be assessed by linear stability analysis, as before. In this case, we obtain

$$\frac{1}{2}\frac{\mathrm{d}}{\mathrm{d}t}|\delta\boldsymbol{u}|^2 = (\delta u_2\, \delta u_3)\begin{bmatrix} \kappa_{22}-\lambda_1 & \kappa_{23} \\ \kappa_{32} & \kappa_{33}-\lambda_1 \end{bmatrix}\begin{pmatrix} \delta u_2 \\ \delta u_3 \end{pmatrix} + o(|\delta\boldsymbol{u}|^2),$$

owing to the orthogonality of $\boldsymbol{U}_e$ and $\delta\boldsymbol{u}$. The eigenvalues of the quadratic form are then computed subject to the assumption of incompressibility of the flow ($\mathrm{tr}\,[\boldsymbol{\kappa}] = 0$); this yields the eigenvalues of $\boldsymbol{U}_e$

$$-\tfrac{3}{2}\lambda_1 \pm \tfrac{1}{2}[(\kappa_{22}-\kappa_{33})^2 + 4\kappa_{23}\kappa_{32}]^{\frac{1}{2}}.$$

By assumption, the term within the square root is negative in case 2. Consequently, the quadratic form is negative definite when $\lambda_1 > 0$; this corresponds to $\boldsymbol{U}_e$ stable. When $\lambda_1 < 0$, $\boldsymbol{U}_e$ is unstable. The asymptotic behaviour of orbits in case 2 is as follows. When $\boldsymbol{U}_e$ is stable (case 2*a*, $\lambda_1 > 0$), then all orbits are attracted to $\boldsymbol{U}_e$ via a spiral trajectory on the surface of the sphere. The periodic solution is an unstable limit cycle. When $\boldsymbol{U}_e$ is unstable (case 2*b*, $\lambda_1 < 0$), then all orbits are attracted to the periodic solution, which is a stable limit cycle.

Remarks on structural stability

Structural stability concerns the robustness of the qualitative dynamics in a dynamical system with respect to small changes in the governing equations. In the analysis of microstructure suspended in simple, two-dimensional flow fields in SWL, it was found that the dynamical behaviour of microstructure is structurally stable only

Case	Eigenvalues (κ)	Attractor	Strong flow criterion
1	$\lambda_1 > \lambda_2 > \lambda_3$	Steady, $\|\boldsymbol{e}_1$	$\lambda_1 > \alpha$
2*a*	$\lambda_1 > 0$ real $\lambda_2 = \bar{\lambda}_3$	Steady, $\|\boldsymbol{e}_1$	$\lambda_1 > \alpha$
2*b*	$\lambda_1 < 0$ real $\lambda_2 = \bar{\lambda}_3$	Limit cycle in a plane	$\frac{1}{T}\int_0^T \boldsymbol{\kappa}:\boldsymbol{u}_{1c}(t)\,\boldsymbol{u}_{1c}(t)\,\mathrm{d}t > \alpha$

TABLE 1. Summary of results in steady flows

in flows where there is a single stable equilibrium, an unstable equilibrium, and a saddle. Such two-dimensional, simple flow fields are an example of case 1. As we have established, there are two other generic possibilities when the flow field is three-dimensional.

3.2. *Stretch of the microstructure*

Now that we understand the generic possibilities for the orientation dynamics of particles in simple three-dimensional flows, we can formulate criteria for stretch of the microstructure. According to (2.5), microstructure that follows the orientation time trace $\boldsymbol{u}(t;\boldsymbol{u}_0)$ in a simple flow will stretch when

$$\frac{G}{T}\int_0^T \boldsymbol{E}:\boldsymbol{u}\boldsymbol{u}(t;\boldsymbol{u}_0)\,\mathrm{d}t > \alpha.$$

It makes sense to apply this criterion to that particular orientation time trace $\boldsymbol{u}(t;\boldsymbol{u}_0)$ which is the unique attractor for the particular simple three-dimensional flow in question. Of course particles may stretch before their orientations reach the attractor; however, specializing our criterion to particles with orientations that lie on the attractor will yield a result that is valid asymptotically in time. If there is a single attracting equilibrium orientation $\boldsymbol{U}_e$, corresponding either to case 1 or to case 2*a*, then the appropriate strong flow criterion is therefore

$$\lambda_1 > \alpha, \tag{3.11}$$

where $\lambda_1 = G\boldsymbol{E}:\boldsymbol{U}_e\boldsymbol{U}_e$ is the eigenvalue of $\boldsymbol{\kappa}$ associated with the eigenvector $\boldsymbol{U}_e$. If there is a stable limit cycle (case 2*b*), then the appropriate strong flow criterion is

$$\frac{G}{T}\boldsymbol{E}:\int_0^T \boldsymbol{u}_{1c}(t)\,\boldsymbol{u}_{1c}(t)\,\mathrm{d}t > \alpha, \tag{3.12}$$

where $\boldsymbol{u}_{1c}(t) = \boldsymbol{u}_{1c}(t+T)$ is the limit cycle of period T. The latter criterion takes into account the history of the orientation dynamics on the attractor. it is interesting to note that history may be important even in a steady flow! For future reference, we summarize in table 1 the results concerning orientation dynamics and strong flow criteria of particles suspended in a three-dimensional flow that is steady in the Lagrangian frame.

Relation to known results for simple flows

In the special case of simple flow, where $\boldsymbol{\kappa}$ is constant, Olbricht *et al.* (1982) obtained the strong flow criterion

$$\mathrm{Re}\,(\lambda) > \alpha. \tag{3.13}$$

Here, λ is the eigenvalue of $\boldsymbol{\kappa}$ with largest real part, and α is the elastic modulus of the microstructure. This criterion corresponds exactly to (3.11) when the attractor is an

equilibrium orientation. However, when the attractor is a limit cycle, the strong flow criterion of Olbricht *et al.* (1982) does not apply, as the history of the motion is not taken into account. Example III, below, is a demonstration of this point.

3.3. *Example I: two-dimensional flows with an attracting equilibrium orientation are structurally stable*

The first example we give demonstrates that the particle dynamical behaviour in two-dimensional flows with an attracting equilibrium orientation is robust. We illustrate this point by adding a small three-dimensional perturbation to such a two-dimensional flow, and observing the changes in particle dynamical behaviour. We shall see that although the attracting equilibrium shifts in the perturbed flow, the qualitative dynamics are unchanged. Of course, the small three-dimensional perturbation is not arbitrary, and so this analysis does not constitute a proof of robustness but merely a demonstration.

We begin with a two-dimensional example flow taken from SWL, §2.2; we set $E_{ij} = 0$ except for $E_{11} = -E_{22} = 3$, and $\Omega_{ij} = 0$ except for $\Omega_{12} = -\Omega_{21} = 2$. When $G = 1$, there is a single attracting equilibrium orientation and a repelling equilibrium orientation in the (x, y)-plane, and a saddle on the z-axis. The phase portrait for the particle orientation dynamics is shown in figure 4 of SWL. The (generic) particle orientation dynamics in this unperturbed flow are therefore an example of case 1 in table 1. Next, we add a small rotational component to the flow about the y-axis, with associated vorticity ϵ:

$$\boldsymbol{\Omega}_\epsilon = \begin{bmatrix} 0 & 0 & -\frac{1}{2}\epsilon \\ 0 & 0 & 0 \\ \frac{1}{2}\epsilon & 0 & 0 \end{bmatrix}.$$

Thus, the full flow $\boldsymbol{\kappa} = G\boldsymbol{E} + \boldsymbol{\Omega} + \boldsymbol{\Omega}_\epsilon$ is slightly three-dimensional for small ϵ.

When $\epsilon \neq 0$, we compute the eigenvalues and eigenvectors of $\boldsymbol{\kappa}$. For $-1.6 \leqslant \epsilon \leqslant 1.6$, we find a stable node, an unstable node and a saddle, together with their symmetric opposites, at every value of ϵ. Thus, all the flows with $-1.6 \leqslant \epsilon \leqslant 1.6$ belong to case 1 of our general analysis. The locations of the equilibria shift as we vary ϵ, as shown in figure 3. However, even after a substantial perturbation of this structurally stable flow the dynamics retains the same character as in the unperturbed flow, i.e. the flow remains an example of case 1.

3.4. *Example II: two-dimensional flows without an attracting equilibrium orientation are structurally unstable*

In the second example, we illustrate the fact that strictly two-dimensional flows without an attractor are structurally unstable. We add a small three-dimensional perturbation to a two-dimensional flow that rotates every initial orientation along a unique periodic trajectory, analogous to the 'Jeffery' orbits of particles in simple shear flow (cf. Jeffery 1922). The slight three-dimensionality changes the asymptotic dynamical behaviour radically from the behaviour in purely two-dimensional flow.

Again we borrow an example from SWL, §2.2; we set $E_{ij} = 0$ except for $E_{11} = -E_{22} = 1$, and $\Omega_{ij} = 0$ except for $\Omega_{12} = -\Omega_{21} = 2$. When $G = 1$, there is no *attracting* equilibrium orientation. There is only a centre on the z-axis. The phase portrait of the particle orientation dynamics in the unperturbed flow is shown in figure 2 of SWL. Clearly, the (non-generic) unperturbed flow is neither an example of case 1 nor of case 2*a* or *b*.

As in Example I, we add $\boldsymbol{\Omega}_\epsilon$, a small rotational component to the flow about the y-axis, with associated vorticity ϵ. As we vary the perturbation vorticity ϵ, the location

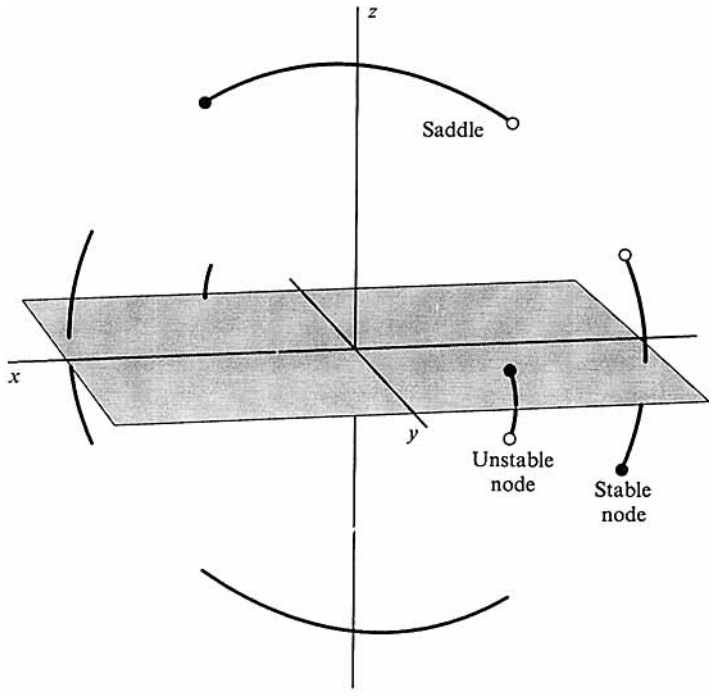

FIGURE 3. Equilibrium orientations of a family of three-dimensional flows that contains a given two-dimensional flow in which the orientation dynamics are structurally stable (Example I). The equilibria are plotted over the parameter range $\epsilon = -1.6$ (open circles) to $\epsilon = 1.6$ (closed circles). Perturbations ($\epsilon \neq 0$) do not change the qualitative nature of the dynamics, which remains an example of case 1 even under a strong perturbation.

of the equilibrium in this family of flows shifts, as shown in figure 4(*a*) for the range $-1.6 \leqslant \epsilon \leqslant 1.6$. It would seem, at first glance, that the unperturbed flow $\boldsymbol{\kappa} = G\boldsymbol{E} + \boldsymbol{\Omega}$ is robust to the perturbation $\boldsymbol{\Omega}_\epsilon$, as the number of equilibria do not change. However, the stability type of the equilibrium does change when $\epsilon \neq 0$. In figure 4(*b*), we plot the (real) eigenvalue that characterizes the stability of the equilibrium orientation (λ_1 of $\boldsymbol{\kappa}$). Note that when $\epsilon = 0$, $\lambda_1 = 0$ corresponding to the centre in the unperturbed flow. When ϵ is different from zero, no matter how slightly, the corresponding equilibrium orientation becomes an attractor, and all the closed trajectories of the unperturbed flow are broken except, of course, for the invariant great circle. Under the perturbation, the non-generic unperturbed flow is transformed into a generic example of case 2*a* of table 1.

An alternate perturbation that produces interesting dynamics is to add

$$\boldsymbol{E}_\epsilon = \begin{bmatrix} -\epsilon & 0 & 0 \\ 0 & -\epsilon & 0 \\ 0 & 0 & 2\epsilon \end{bmatrix}$$

to the basic flow. This corresponds to the addition of a slight uniaxial straining flow when $\epsilon > 0$, or to a slight bi-axial straining flow when $\epsilon < 0$. As ϵ varies we find that, due to the symmetries of this family of flows, the equilibrium orientation remains at $\pm(0, 0, 1)$. However $\lambda_1 = 2\epsilon$; thus, the equilibrium changes from unstable when $\epsilon < 0$ to stable as $\epsilon > 0$, as one might expect. In either case, the closed orbital trajectories of the unperturbed flow are broken for $\epsilon \neq 0$.

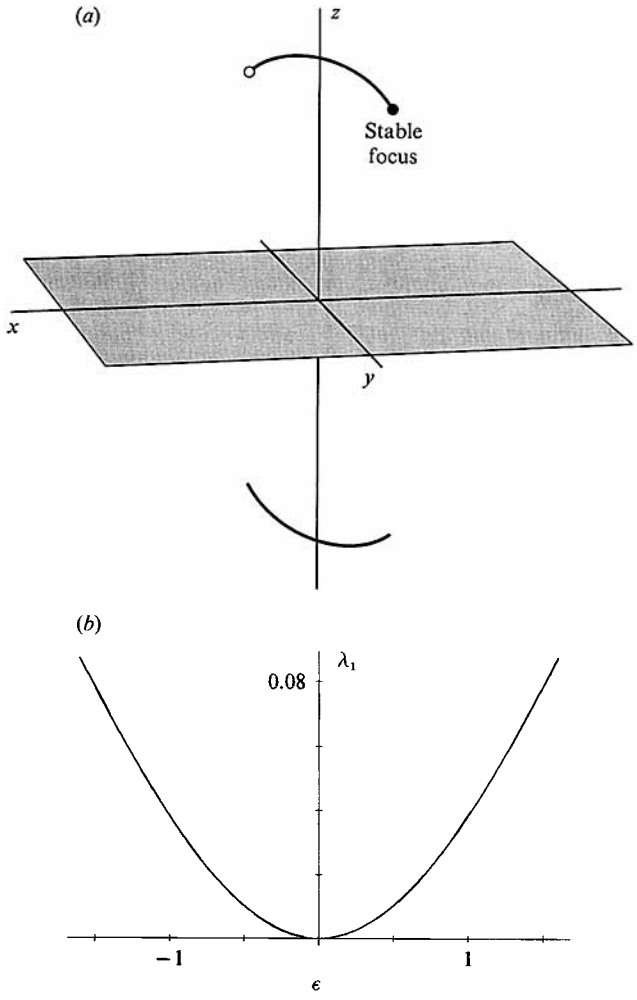

FIGURE 4. (*a*) A plot of the equilibrium orientation of a family of three-dimensional flows that contains a given two−dimensional flow in which the orientation dynamics are structurally unstable (Example II). The equilibria are plotted over the parameter range $\epsilon = -1.6$ (open circles) to $\epsilon = 1.6$ (closed circles). Perturbations ($\epsilon \neq 0$) do not change the number of equilibria, but do change their stability type and therefore also the phase portrait. (*b*) The real eigenvalue (λ_1 of κ) associated with the equilibrium orientation shown in (*a*) versus the parameter ϵ. Note that for $\epsilon \neq 0$, the equilibrium is a stable focus, thus breaking the closed orbital trajectories that exist in the degenerate case $\epsilon = 0$, in which the equilibrium orientation is a centre (metastable).

3.5. *Example III: cases 1 and 2 are connected by saddle-node bifurcation on a limit cycle*

In this third example we consider a family of flows depending on a parameter, such that the flows are examples of case 1 for some values of the parameter, and of case 2 for others. First, we demonstrate that cases 1 and 2 are connected by a special type of global bifurcation, namely a saddle-node bifurcation on a limit cycle. Thompson & Stewart (1986) give a description of this phenomenon, which they refer to as 'omega explosion'. Next, we analyse the stretch degree of freedom in order to see how the stretch depends on the orientation dynamics.

In order to illustrate these points, we construct a 1-parameter family of flows; we set

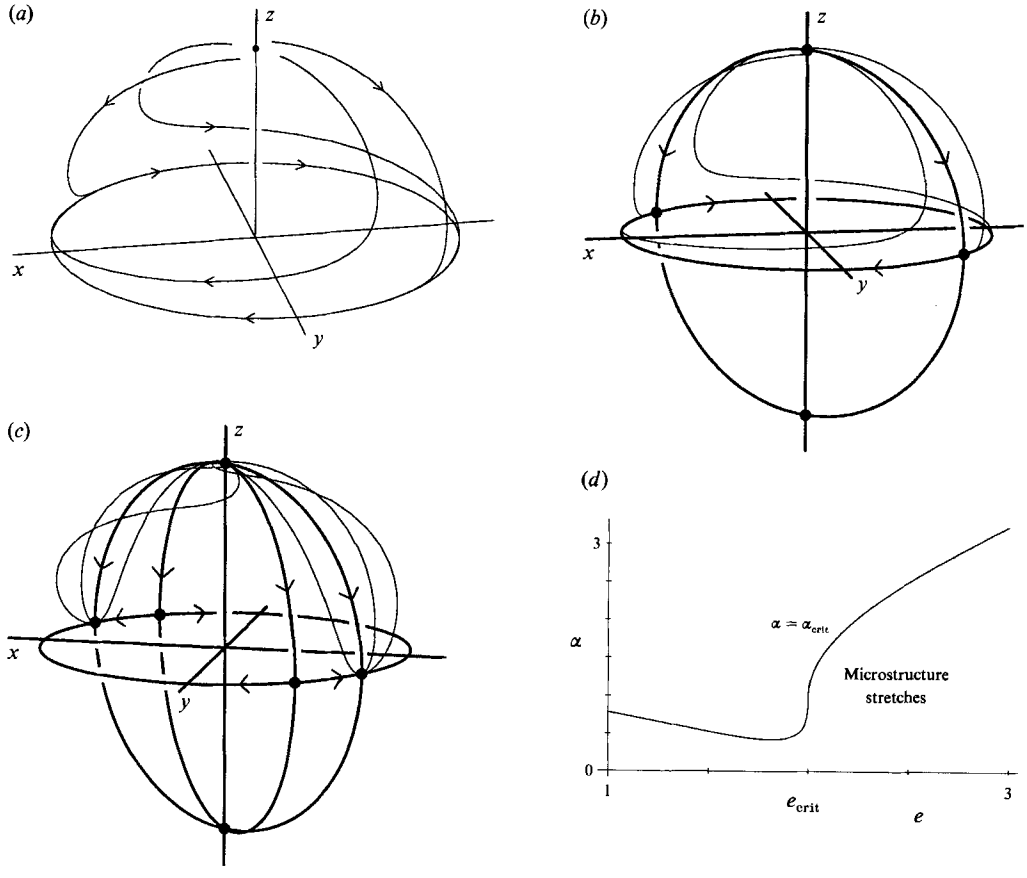

FIGURE 5. (*a*) Phase portrait of the orientation dynamics in the flow of Example III for parameter values that yield case 2*b* dynamics. There is but one (unstable) equilibrium, and a stable limit cycle. (*b*) Phase portrait of the orientation dynamics in the flow of Example III at the bifurcation value of the parameter. There is one unstable equilibrium, a metastable equilibrium, and two invariant great circles. (*c*) Phase portrait of the orientation dynamics in the flow of Example III for parameter values that yield case 1 dynamics. The degenerate orientation of (*b*) has split into a stable orientation and a saddle. There are three invariant great circles. (*d*) A plot of the critical value of the elastic modulus of particles versus the parameter e, for the family of flows of Example III. Note the dramatic transition that occurs at the bifurcation value of the parameter, $e_{crit} = 2$, owing to the catastrophic nature of the global bifurcation there.

$E_{ij} = 0$ except for $E_{11} = -E_{22} = e$, and $\Omega_{ij} = 0$ except for $\Omega_{12} = -\Omega_{21} = 2$, and put $\boldsymbol{\kappa} = G\boldsymbol{E} + \boldsymbol{\Omega} + G\boldsymbol{E}_\epsilon$. We take $G = 1$ hereafter, for simplicity. The eigenvalues of $\boldsymbol{\kappa}$ are

$$2\epsilon, \quad -\epsilon + (e^2-4)^{\frac{1}{2}}, \quad -\epsilon - (e^2-4)^{\frac{1}{2}}.$$

When $e = 1$, this flow is of case 2, with an attracting limit cycle when $\epsilon < 0$ (case 2*b*), and an attracting equilibrium for $\epsilon > 0$ (case 2*a*). When $e = 3$, this is a case 1 flow, with a single attracting equilibrium orientation, a repelling equilibrium orientation, and an equilibrium orientation of saddle type. The critical value of the parameter at which the bifurcation occurs is $e_{crit} = 2$.

In figure 5(*a*), we show the phase portrait for the orientation dynamics when $e = 1.8 < e_{crit}$ (and $\epsilon = -1$). In figure 5(*b*) is the phase portrait at the critical value of the parameter e. Finally, in figure 5*c*, the phase portrait for $e = 2.2$ (and $\epsilon = -1$) shows

that the new saddle and node have appeared on the limit cycle, together with their associated invariant curves. In figure 5(*c*), the attractor is the new, stable node.

In our efforts to quantify stretching of particles in §3.2, we developed strong flow criteria that depend on the type of attractor for the orientation dynamics. As we have observed, the nature of the attractor for the present flow changes from a limit cycle to an equilibrium orientation as e changes from 1 to 3. It is interesting to see how this change is reflected in the stretching characteristics of the flow. Therefore, for $e < e_{\text{crit}}$ (limit cycle), we define the critical elastic modulus for stretch of the microstructure by

$$\alpha_{\text{crit}} \equiv \frac{1}{T}\int_0^T \boldsymbol{\kappa} : \boldsymbol{u}_{\text{lc}}(t)\,\boldsymbol{u}_{\text{lc}}(t)\,\mathrm{d}t$$

from (3.12); when $\alpha < \alpha_{\text{crit}}$ the particle stretches. We define an angular variable σ that serves to parameterize the limit cycle in the (x, y)-plane: $\boldsymbol{u}_{\text{lc}}(t) = (\cos\sigma(t), \sin\sigma(t), 0)$. This is substituted into the evolution equation for $\boldsymbol{u}$, to obtain an equation for σ:

$$(\mathrm{d}/\mathrm{d}t)\,\sigma(t) = -e\sin 2\sigma(t) - 2.$$

This equation is easily integrated to obtain a periodic solution. The critical α is

$$\alpha_{\text{crit}} = \frac{1}{4T}\log\left[\frac{(e^2+4)(e^2-4-16\pi^2)}{(e^2-4)(e^2+8\pi e+4+16\pi^2)}\right] - \epsilon \quad (e < 2).$$

If we take the limit of this expression as e approaches e_{crit} from below, we obtain $\alpha_{\text{crit}} = 1$. Note that this expression is in accord with $\boldsymbol{\kappa} : \boldsymbol{u}_{\text{lc}}\,\boldsymbol{u}_{\text{lc}} = 1 + e\cos(2\sigma)$ evaluated at e_{crit} and at $\sigma = -\frac{1}{4}\pi$, which is the metastable equilibrium that appears on the limit cycle in the global bifurcation at e_{crit}. It is interesting to note that when $e = e_{\text{crit}}$, the stretching power of the flow varies over the limit cycle from $-1 \leqslant \boldsymbol{\kappa} : \boldsymbol{u}_{\text{lc}}\,\boldsymbol{u}_{\text{lc}} \leqslant 3$. Thus, the metastable equilibrium occurs in an orientation that is not the orientation of maximum stretch. Hence, when $e = e_{\text{crit}}$, the microstructure lingers forever in an orientation that is not the orientation of maximum stretching.

For $e > e_{\text{crit}}$, we define the critical elastic modulus to be (cf. (3.11)) $\alpha_{\text{crit}} = \boldsymbol{\kappa} : \boldsymbol{U}_{\text{e}}\,\boldsymbol{U}_{\text{e}}$ where $\boldsymbol{U}_{\text{e}}$ is the stable equilibrium orientation; hence

$$\alpha_{\text{crit}} = (e^2-4)^{\frac{1}{2}} - \epsilon \quad (e > 2).$$

Again, when e approaches e_{crit} from above, the limit of α_{crit} is 1 for $\epsilon = -1$. Note that this equation for α_{crit} is the same that one would obtain from the strong flow criterion of Olbricht *et al.* (1982), which we recalled in (3.13).

For a fixed value of e, the microstructure (on the relevant attractor) will stretch whenever $\alpha < \alpha_{\text{crit}}$. A graph of α_{crit} versus the parameter e for $\epsilon = -1$ is shown in figure 5(*d*). Note the abrupt change in α_{crit} at the bifurcation value e_{crit}. The sensitive nature of the dependence of α_{crit} on e reflects the discontinuous (catastrophic) nature of this bifurcation. In going from $e = 3$ to $e = 1$, there is no hint of the impending catastrophe at e_{crit} to someone observing a particle in the flow. At e_{crit}, the attractor suddenly changes from a steady equilibrium orientation to a limit cycle. In going from $e = 1$ to $e = 3$, the only hint of impending bifurcation is temporal intermittency, in which the orientation on the attractor lingers longer and longer in an almost steady orientation, and then suddenly rotates by almost a full 180°.

4. Time-periodic flows

The dynamics of particles are much richer in flows that are time dependent in the Lagrangian frame, owing to the non-autonomous nature of the orientation and stretch equations in that case. Time-periodic flows are of great significance in applications. For

example, steady, recirculating flows in the Eulerian frame appear time periodic in the Lagrangian frame, when the microstructure follows the same paths as a fluid particle. A second example is a steady flow in a spatially periodic domain such as a wavy-wall tube.

4.1. *Orientation dynamics*

In flows that are T-periodic in the Lagrangian frame associated with an element of the microstructure, the right-hand side of (2.2*a*) is unsteady in orientation space. Rather than study the continuous-time dynamics in orientation space, we examine the Poincaré map of the sphere of orientations to itself. The Poincaré map $\mathscr{P}$ is defined by $\mathscr{P}(\boldsymbol{u}_0) = \boldsymbol{u}(t = T; \boldsymbol{u}_0)$. The map $\mathscr{P}$ is related to the equivalent deformation gradient tensor $\boldsymbol{Q}$, evaluated at the period of the flow T, by the equation

$$\mathscr{P}(\boldsymbol{u}_0) \equiv \boldsymbol{u}(T; \boldsymbol{u}_0) = \frac{\boldsymbol{Q}(T) \cdot \boldsymbol{u}_0}{|\boldsymbol{Q}(T) \cdot \boldsymbol{u}_0|}. \tag{4.1}$$

Fixed points of the Poincaré map $\boldsymbol{U}_T$ correspond to time-periodic solutions of the underlying differential equation; thus $\boldsymbol{u}(t+T; \boldsymbol{U}_T) = \boldsymbol{u}(t; \boldsymbol{U}_T)$. Moreover, fixed points of $\mathscr{P}$ are eigenvectors of the equivalent deformation gradient tensor $\boldsymbol{Q}$, evaluated at the period of the flow T, with corresponding eigenvalue $|\boldsymbol{Q}(T) \cdot \boldsymbol{U}_T|$.

A major difference from the simple flow case is that $\boldsymbol{Q}(T)$ and $\boldsymbol{\kappa}$ do not have a common set of eigenvectors, in general. The eigenvalue of $\boldsymbol{Q}(T)$ associated with $\boldsymbol{U}_T$ can be related to the tensor $\boldsymbol{\kappa}$ as follows. We take the product of (2.3) with $\boldsymbol{U}_T$ and make use of (2.4) to obtain

$$(\mathrm{d}/\mathrm{d}t)\, \boldsymbol{Q}(t) \cdot \boldsymbol{U}_T = \boldsymbol{\kappa}(t) \cdot \boldsymbol{u}(t; \boldsymbol{U}_T) |\boldsymbol{Q}(t) \cdot \boldsymbol{U}_T|.$$

This result is used to derive

$$\begin{aligned}(\mathrm{d}/\mathrm{d}t) |\boldsymbol{Q}(t) \cdot \boldsymbol{U}_T| &= \boldsymbol{u}(t; \boldsymbol{U}_T) \cdot (\mathrm{d}/\mathrm{d}t)\, \boldsymbol{Q}(t) \cdot \boldsymbol{U}_T \\ &= \boldsymbol{u}(t; \boldsymbol{U}_T) \cdot \boldsymbol{\kappa}(t) \cdot \boldsymbol{u}(t; \boldsymbol{U}_T) |\boldsymbol{Q}(t) \cdot \boldsymbol{U}_T|.\end{aligned}$$

This equation may be integrated to obtain the solution

$$|\boldsymbol{Q}(T) \cdot \boldsymbol{U}_T| = \exp \int_0^T \boldsymbol{u}(\tau; \boldsymbol{U}_T) \cdot \boldsymbol{\kappa}(\tau) \cdot \boldsymbol{u}(\tau; \boldsymbol{U}_T)\, \mathrm{d}\tau. \tag{4.2}$$

Thus, the eigenvalue of $\boldsymbol{Q}(T)$ associated with the eigenvector $\boldsymbol{U}_T$ takes into account the history of the flows and orientations experienced by a particle which follows the periodic orbit associated with $\boldsymbol{U}_T$. Note that eigenvalues of $\boldsymbol{Q}(T)$ corresponding to real eigenvectors $\boldsymbol{U}_T$ must be positive, as they are exponentials of finite quantities.

The dynamics of $\mathscr{P}$ are thus related to the properties of generic, second-rank tensors $\boldsymbol{Q}(T)$. Thus, our arguments in this section will be of a similar form to those in §3. One major difference is that the eigenvectors associated with real eigenvalues of $\boldsymbol{Q}(T)$ are fixed points of the Poincaré map $\mathscr{P}$, and therefore correspond to periodic orientations with period T. We analyse the two generic types of behaviour in turn.

Case 1: $\boldsymbol{Q}(T)$ has three distinct, real, positive eigenvalues.

In this case, there are three eigenvectors, or fixed points of the Poincaré map, $\boldsymbol{U}_T^{(i)}$, $i = 1, 2, 3$. By Schur's theorem, $\boldsymbol{Q}(T)$ may be written as an upper triangular matrix with the (constant) eigenvalues ξ_i appearing on the diagonal. Then the Poincaré map $\mathscr{P}$ may be written

$$\mathscr{P}\begin{pmatrix} u_1 \\ u_2 \\ u_3 \end{pmatrix} = \left| \begin{bmatrix} \xi_1 & Q_{12} & Q_{13} \\ 0 & \xi_2 & Q_{23} \\ 0 & 0 & \xi_3 \end{bmatrix} \begin{pmatrix} u_1 \\ u_2 \\ u_3 \end{pmatrix} \right|^{-1} \begin{bmatrix} \xi_1 & Q_{12} & Q_{13} \\ 0 & \xi_2 & Q_{23} \\ 0 & 0 & \xi_3 \end{bmatrix} \begin{pmatrix} u_1 \\ u_2 \\ u_3 \end{pmatrix}. \tag{4.3}$$

By analysis of (4.3), one can show that there are three invariant great circles of the Poincaré map on the sphere of orientations. Hence, a particle orientation which begins on one of the invariant great circles will return to the same invariant great circle at every period of the flow, *ad infinitum*. The invariant great circles lie on planes normal to the vectors given by (3.7) with ξ_i substituted for λ_i, and Q_{ij} substituted for κ_{ij}. The fixed points of the Poincaré map are at the (six) intersections of these great circles; the associated periodic orbits pass through the fixed points at every multiple of the period of the flow. These points are given by the orientations $\boldsymbol{U}_T^{(i)}$, which are identical to $\boldsymbol{U}_e^{(i)}$ of (3.8) with ξ_i substituted for λ_i, and Q_{ij} substituted for κ_{ij}.

The stability of a fixed point may be determined by a linear stability analysis of the Poincaré map about the fixed point, as follows. First, we compute the derivative of $\mathscr{P}$

$$\frac{\mathrm{d}}{\mathrm{d}\epsilon}\mathscr{P}(\boldsymbol{u}_0+\epsilon\delta\boldsymbol{u}_0)\bigg|_{\epsilon=0} = \mathrm{D}_u\mathscr{P}(\boldsymbol{u}_0)\cdot\delta\boldsymbol{u}_0 = \frac{1}{|\boldsymbol{Q}(T)\cdot\boldsymbol{u}_0|}[\boldsymbol{I}-\boldsymbol{u}_0\otimes\boldsymbol{u}_0]\cdot\boldsymbol{Q}(T)\cdot\delta\boldsymbol{u}_0,$$

where D_u is the derivative with respect to $\boldsymbol{u}$, i.e. the gradient operator on the sphere of orientations, and $\delta\boldsymbol{u}_0 = (\delta u_1^{(0)}, \delta u_2^{(0)}, \delta u_3^{(0)})$. Now we consider the stability of $\boldsymbol{U}_T^{(1)}$. Because $\boldsymbol{u}$ is a unit vector, we must have $\boldsymbol{U}_T^{(1)}\cdot\delta\boldsymbol{u}_0 = 0$; hence $\delta u_1^{(0)} = 0$. The linearized Poincaré map may be written

$$\mathrm{D}_u\mathscr{P}(\boldsymbol{U}_T^{(1)})\cdot\delta\boldsymbol{u}_0 = \frac{1}{|\boldsymbol{Q}(T)\cdot\boldsymbol{U}_T^{(1)}|}\begin{bmatrix}\xi_2 & Q_{23}\\ 0 & \xi_3\end{bmatrix}\begin{pmatrix}\delta u_2^{(0)}\\ \delta u_3^{(0)}\end{pmatrix} = \begin{bmatrix}\xi_2/\xi_1 & Q_{23}/\xi_1\\ 0 & \xi_3/\xi_1\end{bmatrix}\begin{pmatrix}\delta u_2^{(0)}\\ \delta u_3^{(0)}\end{pmatrix}.$$

Bearing in mind that $\xi_1\xi_2\xi_3 = \det[\boldsymbol{Q}(T)] = 1$, $\boldsymbol{U}_T^{(1)}$ has the following stability type: if $\xi_1 > \xi_2 > \xi_3$, $\boldsymbol{U}_T^{(1)}$ is a stable node, if $\xi_1 < \xi_2 < \xi_3$, $\boldsymbol{U}_T^{(1)}$ is an unstable node, and if $\xi_2 < \xi_1 < \xi_3$ or $\xi_3 < \xi_1 < \xi_2$, $\boldsymbol{U}_T^{(1)}$ is a saddle point of the Poincaré map. Thus, the eigenvector associated with the maximum eigenvalue of $\boldsymbol{Q}(T)$ is the unique attractor for the Poincaré map. The associated periodic integral curve of (2.2*a*) is the unique attractor in the system of underlying equations.

The asymptotic behaviour of microstructure in time-periodic flows where the equivalent deformation gradient tensor $\boldsymbol{Q}(T)$ has three real, distinct eigenvalues is as follows. As before, the sphere of orientations is divided into spherical triangular cells; the cell boundaries are boundaries of the orbits of points under the map. Within each cell, orbits tend to the unstable node under backward iterates of the Poincaré map, and to the stable node under forward iterates of the map; this situation corresponds to phase locking. After an initial transient, the microstructure in a case 1 flow settles down onto a periodic attractor, with the same period as the time-periodic flow. In addition, the 'phases' of all initial orientations are identical as they become phase locked with the forcing. In effect, each particle forgets its initial orientation.

Case 2: $\boldsymbol{Q}(t)$ has one real, non-zero eigenvalue, and a complex-conjugate pair.

In case 2, there is but one fixed point of the Poincaré map $\mathscr{P}$, $\boldsymbol{U}_T$ associated with the real eigenvalue ξ_1. We make use of Schur's theorem and write the Poincaré map $\mathscr{P}$ in the form

$$\mathscr{P}\begin{pmatrix}u_1\\ u_2\\ u_3\end{pmatrix} = \left|\begin{bmatrix}\xi_1 & Q_{12} & Q_{13}\\ 0 & Q_{22} & Q_{23}\\ 0 & Q_{32} & Q_{33}\end{bmatrix}\begin{pmatrix}u_1\\ u_2\\ u_3\end{pmatrix}\right|^{-1}\begin{bmatrix}\xi_1 & Q_{12} & Q_{13}\\ 0 & Q_{22} & Q_{23}\\ 0 & Q_{32} & Q_{33}\end{bmatrix}\begin{pmatrix}u_1\\ u_2\\ u_3\end{pmatrix}. \tag{4.4}$$

We require $$4Q_{23}Q_{32} < -(Q_{22}-Q_{33})^2,$$

to ensure that the remaining eigenvalues are a complex conjugate pair. In case 2, there is a single invariant great circle, which lies in the plane normal to the vector given by

(3.10) with ξ_1 substituted for λ_1, and Q_{ij} substituted for κ_{ij}. Also, there is a fixed orientation $\boldsymbol{U}_T = \pm(1,0,0)$. The fixed point is not contained in the invariant great circle, and so the circle is associated with a (generally) quasi-periodic motion in the system, by the following arguments. Consider an initial orientation that lies on the invariant great circle. This orientation will map to another orientation that lies on the invariant great circle after one period of the flow, and so on. Future iterates will make their way around the invariant great circle without stopping. After some number of forward iterates of the Poincaré map, the point will eventually pass all the way around the invariant great circle, and so will pass through the initial orientation and on to a second circumnavigation of the great circle. This process continues indefinitely. In the very special case where some future iterate of the initial orientation coincides exactly with the initial orientation, say $\mathscr{P}^m(\boldsymbol{u}_0) = \boldsymbol{u}_0 (m > 1)$, then that initial orientation is m-periodic in the map, and also in the underlying differential equation, where the solution has the property $\boldsymbol{u}(t;\boldsymbol{u}_0) = \boldsymbol{u}(t+mT;\boldsymbol{u}_0)$. Otherwise, the dynamics are quasi-periodic, and the integral curve $\boldsymbol{u}(t;\boldsymbol{u}_0)$ never repeats itself. We consider the fate of orientations that are not initially on the invariant great circle after analysing the stability of the fixed point of the map.

The stability of the fixed orientation $\boldsymbol{U}_T$, and of the associated periodic integral curve $\boldsymbol{u}(t;\boldsymbol{U}_T)$ is assessed as before. The linearization of $\mathscr{P}$ is

$$\mathrm{D}_u\mathscr{P}(\boldsymbol{U}_T)\cdot\delta\boldsymbol{u}_0 = \frac{1}{\xi_1}\begin{bmatrix} Q_{22} & Q_{23} \\ Q_{32} & Q_{33} \end{bmatrix}\begin{pmatrix} \delta u_2^{(0)} \\ \delta u_3^{(0)} \end{pmatrix},$$

with eigenvalues

$$\frac{1}{2\xi_1}[(Q_{22}+Q_{33}) \pm ((Q_{22}-Q_{33})^2 + 4Q_{23}Q_{32})^{\frac{1}{2}}].$$

By assumption, the term within the square root is negative; thus the eigenvalues are complex conjugates with modulus square

$$\frac{1}{\xi_1^2}\det\begin{bmatrix} Q_{22} & Q_{23} \\ Q_{32} & Q_{33} \end{bmatrix}.$$

Now, this determinant is equal to the product of the eigenvalues of the matrix

$$\begin{bmatrix} Q_{22} & Q_{23} \\ Q_{32} & Q_{33} \end{bmatrix},$$

which are the remaining eigenvalues in the spectrum of $\boldsymbol{Q}(T)$ after removal of $\{\xi_1\}$. The product of all three eigenvalues of $\boldsymbol{Q}(T)$ is 1. Therefore, the modulus square of the eigenvalues of the linearization of the Poincaré map at the single fixed orientation $\boldsymbol{U}_T$ is $1/\xi_1^3$. Hence, $\xi_1 > 1$ corresponds to $\boldsymbol{U}_T$ stable, and $\xi_1 < 1$ to $\boldsymbol{U}_T$ unstable.

Thus, we have established that there are two generic types of asymptotic behaviour in time-periodic, three-dimensional flow fields. Either the microstructure is phase locked (case 1 or case 2*a* ($\xi_1 > 1$)); or, the microstructure tumbles in a quasi-periodic fashion (case 2*b* with $\xi_1 < 1$).

Bifurcations of orientation dynamics in time-periodic flows

In Example III, we considered a family of steady flows depending on a parameter that produce dynamics of case 1 for some parameter values and case 2 for others. These two types of dynamical behaviour are connected by a saddle-node bifurcation on the limit cycle of the case 2 flow. In time-periodic flows, the dynamics can undergo a similar bifurcation.

A case 2 time-periodic flow, in which the Poincaré map for orientation dynamics has a fixed orientation and an invariant curve, is connected to a case 1 flow, in which there are three fixed orientations, by a saddle-node bifurcation of the Poincaré map on the invariant great circle of the case 2 flow. In this way, the orientation dynamics can bifurcate from phase-locked to quasi-periodic behaviour (or the reverse) as one varies a parameter. The latter is an example of intermittency and entrainment; we refer the reader to Thompson & Stewart (1986) for a general discussion. As we have seen in Example III, when the attractor for the orientation dynamics changes abruptly, there are important ramifications for the stretch of particles, to which we now turn our attention.

4.2. *Stretch of the microstructure*

We have argued that it is most sensible to develop strong flow criteria based on integration of (2.5) on the attractor. One must keep in mind, however, that stretch may occur during the initial transient in the orientation dynamics. When there is a stable fixed point of the Poincaré map, there is a periodic attractor for the orientation dynamics. The fixed point, in turn, is related to an eigenvector $\boldsymbol{U}_T$ of the equivalent deformation gradient tensor $\boldsymbol{Q}(T)$ evaluated at a period of the flow, with associated eigenvalue $\xi_1 > 1$. We therefore combine (2.5) and (4.2) in order to obtain the strong flow criterion

$$(1/T)\log \xi_1 > \alpha, \tag{4.5}$$

that relates ξ_1 and the period of the flow T to the elastic modulus of the particle α. Recall from our previous arguments that the eigenvalue ξ_1 characterizes the stability of the periodic integral curve. Clearly, the strong flow criterion can only be satisfied when the periodic integral curve is an attractor ($\xi_1 > 1$). Hence the eigenvalue ξ_1 determines both the stability of the associated eigenvector, and the total stretching capacity of the flow for particles that follow the attracting integral curve. The criterion (4.5) is in accord with our previous results for time-periodic, two-dimensional flows presented in SWL. This may be shown by deriving (4.5) in spherical polar coordinates, and restricting to two-dimensional flows.

Now we turn to the situation when the attractor is quasi-periodic. In this case, the solution of the stretch equation (2.5) is considerably more complicated, even for particles with orientations on the attractor. Indeed, it is possible for the attracting integral curve to be dense in some subset (or all) of the sphere of orientations. This means that at any instant of time, the associated integral curve of the orientation (on the attractor) could take on any one of a whole distribution of possible orientations. We emphasize that the integral curve is deterministic, but it may visit whole regions of orientation space over a sufficiently long interval of time. Hence the history of the orientations experienced by the particle is not simple to compute, as it is when the attractor for orientation dynamics is simply periodic. This will be clear in Example IV in §4.3. With this in mind, it seems that when the attractor is quasi-periodic it is more fruitful to consider sufficient conditions for no stretch of the particle on a given path. This leads to weak flow criteria, to which we return in §6. We summarize the results obtained in §4 so far in table 2.

4.3. *Example IV: an almost two-dimensional flow with a wobbling vorticity axis*

The results of §§4.1 and 4.2 apply to nearly two-dimensional flows as well as to fully three-dimensional flows; in this example we consider a three-dimensional flow comprised of a two-dimensional flow with a vorticity axis that wobbles slightly in a time in a periodic fashion. Thus, the flow is nearly two-dimensional, and is meant to

Case	Eigenvalues ($\boldsymbol{Q}$)	Attractor	Strong flow criterion
1	$\xi_1 > \xi_2 > \xi_3$	Limit cycle	$\frac{1}{T}\log\xi_1 > \alpha$
2*a*	$\xi_1 > 1$ real $\xi_2 = \bar{\xi}_3$	Limit cycle	$\frac{1}{T}\log\xi_1 > \alpha$
2*b*	$\xi_1 < 1$ real $\xi_2 = \bar{\xi}_3$	Quasi-periodic (in plane with T-periodic normal)	?

TABLE 2. Summary of results in periodic flows

model what might happen in a particle dynamics experiment conducted in a faulty 'two-dimensional' flow device. The flow we consider is a piecewise constant, periodic flow consisting of

$$\boldsymbol{\kappa}^{(1)} = \begin{bmatrix} 1 & 2 & 0 \\ -2 & -1 & 0 \\ 0 & 0 & 0 \end{bmatrix}, \quad nT \leqslant t < (n+\tfrac{1}{2})T, \tag{4.6a}$$

and

$$\boldsymbol{\kappa}^{(2)} = \boldsymbol{\Theta}\cdot\boldsymbol{\kappa}^{(1)}\cdot\boldsymbol{\Theta}^{\mathrm{T}}, \quad (n+\tfrac{1}{2})T \leqslant t < (n+1)T, \tag{4.6b}$$

where the multiplication by

$$\boldsymbol{\Theta} = \begin{bmatrix} \cos\theta & 0 & \sin\theta \\ 0 & 1 & 0 \\ -\sin\theta & 0 & \cos\theta \end{bmatrix} \tag{4.6c}$$

has the effect of rotating the vorticity axis of $\boldsymbol{\kappa}^{(1)}$ by the angle θ with respect to the 2-axis. The piecewise-constant flow field allows us to integrate the equivalent deformation gradient tensor analytically. Physically, one might imagine that this example corresponds to a flow field that changes continuously in time, but on a timescale that is much shorter than the response time of a particle.

The solution for the orientation dynamics is obtained as follows. We integrate (2.3) over the two subintervals independently. Over the first subinterval, we have the solution

$$\boldsymbol{Q}^{(1)} = \begin{bmatrix} \cos\sqrt{3}t + \dfrac{1}{\sqrt{3}}\sin\sqrt{3}t & \dfrac{2}{\sqrt{3}}\sin\sqrt{3}t & 0 \\ \dfrac{-2}{\sqrt{3}}\sin\sqrt{3}t & \cos\sqrt{3}t - \dfrac{1}{\sqrt{3}}\sin\sqrt{3}t & 0 \\ 0 & 0 & 1 \end{bmatrix}.$$

Over the second subinterval, one can show

$$\boldsymbol{Q}^{(2)}(T) = \boldsymbol{\Theta}\cdot\boldsymbol{Q}^{(1)}(\tfrac{1}{2}T)\cdot\boldsymbol{\Theta}^{\mathrm{T}}.$$

We concatenate the solution over the two subintervals to obtain the Poincaré map:

$$\boldsymbol{u}(T;\boldsymbol{u}_0) = \mathscr{P}(\boldsymbol{u}_0) = \frac{\boldsymbol{Q}^{(2)}(T)\cdot\boldsymbol{Q}^{(1)}(\frac{1}{2}T)\cdot\boldsymbol{u}_0}{|\boldsymbol{Q}^{(2)}(T)\cdot\boldsymbol{Q}^{(1)}(\frac{1}{2}T)\cdot\boldsymbol{u}_0|}.$$

The only free parameters in our flow are the angle of wobble θ and the period of wobble T. Hereafter, we fix the angle of wobble $\theta = \pi/30 = 6°$. As we vary the period

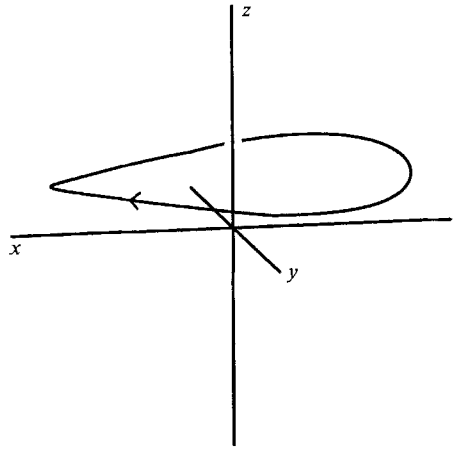

FIGURE 6. Time trace of the periodic attractor of Example IV when $T = 3.6$.

of the wobble T, we find the following behaviour. For all values of T we investigated ($0 < T < 20$), the periodic flow is of case 2; i.e. there is always a single fixed orientation of the Poincaré map and an invariant great circle. The fixed point is stable (case 2*a*), and the invariant circle unstable when

$$T \in p \equiv \{0 < T \leqslant 3.628\} \cup \{7.255 < T \leqslant 10.88\} \cup \{14.51 < T \leqslant 18.14\}.$$

Otherwise, in the interval $q = \{0 < T < 20\} - p$, the fixed point is unstable (case 2*b*) and the invariant curve stable. Thus, when T is in p, the attractor is periodic, and when T is in q, the attractor is quasi-periodic. Presumably, there is some dependence of these intervals on wobble angle θ, but this we chose not to pursue.

It is interesting to note that the period of rotation of a particle in either $\boldsymbol{\kappa}^{(1)}$ (steady) or $\boldsymbol{\kappa}^{(2)}$ (steady) is $T_{\text{rot}} = 1.8138$, which is half the length of the parameter intervals that comprise p. In other words, we have

$$p = \{0 < T \leqslant 2T_{\text{rot}}\} \cup \{4T_{\text{rot}} < T \leqslant 6T_{\text{rot}}\} \cup \{8T_{\text{rot}} < T \leqslant 10T_{\text{rot}}\}.$$

From a physical point of view, we see that the response of the particle in the time-periodic flow depends on the relationship between the timescale for particle response and the timescale of the forcing.

Now, let us examine some integral curves corresponding to each type of attractor. In figure 6, we show the periodic attractor when $T = 3.6$ (in the set p). The initial point on the periodic attractor is $\boldsymbol{u}_0 = (-0.017\,536\,7, 0.968\,394, 0.248\,809)$. Note that the periodic attractor in this case is not a great circle, as is an attracting limit cycle for orientation dynamics in a simple flow. Moreover, the asymptotic dynamics on this attracting integral curve are phase locked, meaning that the phase on the periodic attractor does not depend on initial orientation. This is different from the dynamics on a limit cycle in steady flow. Evaluation of the strong flow criterion (4.5) yields the critical elastic modulus $\alpha_{\text{crit}} = 0.007\,18$.

When $T = 3.7$ (in the set q), we see markedly different dynamics on the attractor. In order to observe dynamics on the quasi-periodic attractor, we must find an initial orientation on the attractor; we do this as follows. First, we compute the normal to the invariant plane, which is $\boldsymbol{n} = (-0.098\,025\,1, -0.848\,882, 0.519\,413)$. Next, we compute a point on the intersection of the sphere of orientations with the invariant plane (i.e. on the invariant great circle of the Poincaré map). Of course, there are an infinite

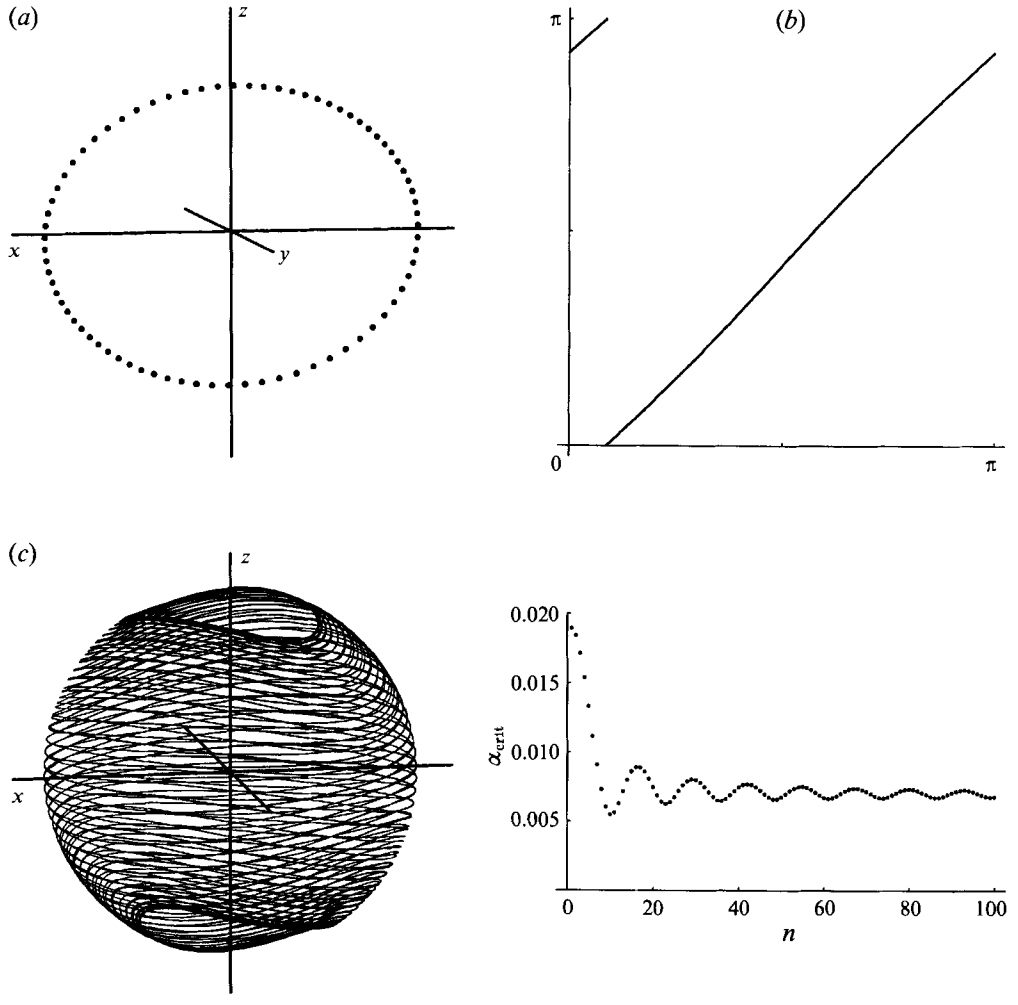

FIGURE 7. (*a*) 100 Iterates of the Poincaré map of the point $\boldsymbol{u}_0 = (0.982654, 0, 0.185449)$ on the invariant circle, for the flow of Example IV with $T = 3.7$. (*b*) A graph of the reduced Poincaré map on the invariant great circle of Example IV when $T = 3.7$. (*c*) Time trace of a part of the quasi-periodic attractor of Example IV when $T = 3.7$ shown in (*a*). The time interval of the calculation was 100 periods. (*d*) The critical elastic modulus (defined as in Example III) of a particle that follows the time trace of (*c*) for n periods.

number of such points. Therefore, we choose the point with y-coordinate zero and obtain $\boldsymbol{u}_0 = (0.982654, 0, 0.185449)$. If we take 100 iterates of the orientation $\boldsymbol{u}_0$, we obtain figure 7(*a*). In this figure, the invariant great circle is clearly visible. The greater the number of iterates one computes, the more filled the circle becomes†. One can restrict the Poincaré map to the circle and obtain the (reduced) circle map shown in figure 7(*b*).

The time trace corresponding to the orbit shown in figure 7(*a*) is shown in figure 7(*c*). Note that a very large portion of the sphere of orientations is visited by this particle in a periodic three-dimensional flow, although it seems that the regions near the 'poles'

† In a numerical calculation such as this one, however, it is impossible to tell whether this is truly a case of multiple, incommensurate frequencies in the response, or rather a strictly periodic response of period mT, where m is a large integer.

are avoided. If we carry out this calculation for a longer time, the visited portion of the sphere is more densely filled. Obviously, the history of the orientations on the attractor (which do have a phase dependence on initial conditions) is extremely complicated. It is for this reason that we were unable to give a well-defined strong flow criterion for case 2*b* of table 2. However, it is possible to compute a critical α for a trajectory that follows the attractor for a finite time. For the trajectory shown in figure 7(*c*), the critical α below which a particle will stretch is shown in figure 7(*d*). Note the difference in behaviour over the first few iterates and in the long term. It is exactly this very complicated history of orientations experienced by the particle that prevents us from formulating a well-defined strong flow criterion when the attractor is quasi-periodic.

We remark that the global, geometric features of these complicated dynamics in the Lagrangian frame are considered in detail by Szeri (1993).

5. Flows with general time-dependence

In the interest of completeness, we consider briefly microstructure suspended in three-dimensional flows with general time-dependence; this is a relatively straightforward extension of the analysis of §4. In what follows, we shall consider particle dynamics over a time interval of interest, $0 \leqslant t \leqslant T$, where T is chosen so as to include interesting features of the flow.

The solution to the orientation dynamics problem may still be represented in the form (2.4). Consequently, there will in general be either one or three fixed orientations of the map

$$\boldsymbol{u}_0 \mapsto \boldsymbol{u}(T;\boldsymbol{u}_0) = \frac{\boldsymbol{Q}(T)\cdot\boldsymbol{u}_0}{|\boldsymbol{Q}(T)\cdot\boldsymbol{u}_0|}. \tag{5.1}$$

If there is a single fixed orientation for the map (5.1) ($\boldsymbol{U}_{\text{fixed}}$) then nearby orientations approach the integral curve $\boldsymbol{u}(t;\boldsymbol{U}_{\text{fixed}})$ if the eigenvalue of $\boldsymbol{Q}(T)$ associated with $\boldsymbol{U}_{\text{fixed}}$ ($|\boldsymbol{Q}(T)\cdot\boldsymbol{U}_{\text{fixed}}|$) is less than one. Nearby orientations diverge over the time interval if the eigenvalue is greater than one. Note that we cannot conclude true stability or instability of the integral curve $\boldsymbol{u}(t;\boldsymbol{U}_{\text{fixed}})$ by these arguments, because we can only treat finite time intervals. If there are three fixed orientations for the map (5.1) over the interval $0 \leqslant t \leqslant T$, the integral curve passing through the eigenvector of $\boldsymbol{Q}(T)$ associated with the maximum eigenvalue attracts nearby orientations over the time interval.

As in §§3 and 4, it is possible to relate the dynamics in the stretch degree of freedom to the equivalent deformation gradient tensor $\boldsymbol{Q}(T)$. We use the map (5.1) and the result (4.2), which also applies in the present context, to derive a history-dependent strong flow criterion

$$\max_{|\boldsymbol{u}_0|=1} \frac{1}{T}\log|\boldsymbol{Q}(T)\cdot\boldsymbol{u}_0| > \alpha. \tag{5.2}$$

This completely general criterion accounts for the history of flows experienced by the particle, as well as the history of the orientation dynamics of the particle. The criterion may be specialized to flows that are steady or time periodic from the point of view of the particles, in which case the earlier criteria we developed, (3.11), (3.12), (4.5), emerge. In practice, it may be more useful to apply the sufficient conditions for weak flow that we derive in the next section.

6. Weak flow criteria in the absence of detailed information

History-dependent strong flow criteria may be cumbersome to apply in some practical situations since both detailed knowledge of the orientation dynamics of the microstructure and of particle paths in the flow are required. Moreover, strong flow criteria may be impractical in cases where the attracting set for orientation dynamics is complicated, e.g. quasi-periodic. These practical considerations motivate the analysis of this section.

6.1. *Sufficient conditions along a particle path*

First, consider the necessary and sufficient condition for a flow to stretch microstructure in some initial orientation along a given particle path, the general history-dependent strong flow criterion (that may be derived from (2.5)),

$$\max_{|\boldsymbol{u}_0|=1} \frac{1}{T} \int_0^T \boldsymbol{\kappa}(t) : \boldsymbol{u}(t;\boldsymbol{u}_0)\,\boldsymbol{u}(t;\boldsymbol{u}_0)\,\mathrm{d}t > \alpha. \tag{6.1}$$

We shall bound the integral in (6.1) using the properties of the rate-of-strain tensor. At any instant of time t, the rate-of-strain tensor has eigenvalues $s_1(t)$, $s_2(t)$ and $s_3(t)$, which sum to zero if the flow is incompressible. Let us suppose that these are ordered so that $s_1 \geqslant s_2 \geqslant s_3$ for all $0 \leqslant t \leqslant T$; thus $s_1(t) \geqslant 0$ and $s_3(t) \leqslant 0$ over the time interval. At any instant of time t, the integrand of (6.1) may be bounded by the inequalities

$$Gs_3(t) \leqslant \boldsymbol{\kappa}(t) : \boldsymbol{u}(t;\boldsymbol{u}_0)\,\boldsymbol{u}(t;\boldsymbol{u}_0) \leqslant Gs_1(t). \tag{6.2}$$

These bounds are obtained simply by evaluating the integrand in the directions ($\boldsymbol{u}$) where it is maximum and minimum, i.e. in the directions of the (instantaneous) eigenvectors of $\boldsymbol{E}$ corresponding to $s_1(t)$ and $s_3(t)$, respectively. The important thing to note about the bounds is that the dependence on the orientation dynamics $\boldsymbol{u}(t;\boldsymbol{u}_0)$ is avoided.

Along a given particle path, it is a simple matter to bound the integral in (6.1) by

$$\frac{G}{T}\int_0^T s_3(t)\,\mathrm{d}t \leqslant \max_{|\boldsymbol{u}_0|=1} \frac{1}{T}\int_0^T \boldsymbol{\kappa}(t) : \boldsymbol{u}(t;\boldsymbol{u}_0)\,\boldsymbol{u}(t;\boldsymbol{u}_0)\,\mathrm{d}t \leqslant \frac{G}{T}\int_0^T s_1(t)\,\mathrm{d}t.$$

Thus, there can be no stretch of the microstructure if

$$\frac{1}{T}\int_0^T s_1(t)\,\mathrm{d}t < \frac{\alpha}{G}. \tag{6.3}$$

In words, there can be no stretch of the microstructure along a particle path on which the average of the maximum eigenvalue of the rate-of-strain tensor is too small. This weak flow criterion retains the history of the flows experienced by the microstructure on a given path, but disregards the history of the orientation dynamics of the microstructure in favour of a simpler, but more conservative, criterion.

6.2. *Sufficient conditions in a region*

Additionally, one can derive a weak flow criterion that applies to regions of flow, thus disregarding the history of the flows experienced by the microstructure in order to obtain an even simpler (and even more conservative) criterion. Consider a fixed (spatial) region A in the domain of the flow; A might be a region bounded by an envelope of closed particle paths in a recirculating flow, for example. Suppose further that the maximum eigenvalue of the rate-of-strain tensor anywhere in A is $s_{\max}$. Then

along any particle path which lies in the region A during the time interval $0 \leqslant t \leqslant T$, we have an upper bound for the integral on the left-hand side of the inequality (6.3): $s_{\max}$. Thus if

$$s_{\max} < \alpha/G, \tag{6.4}$$

there can be no particle path lying wholly in A on which there is a net stretch of the microstructure over the interval $0 \leqslant t \leqslant T$.

7. Conclusions

In this paper, we have analysed the dynamical behaviour of microstructure in three-dimensional flow fields that are steady and time dependent in the Lagrangian frame of the microstructure. We paid particular attention to generic behaviour, as that is what one would expect to find in a physical flow. The exception is our discussion of bifurcations that connect different generic flows through a non-generic flow.

In steady flows, orientation dynamics are characterized by the presence of either a unique, globally attracting equilibrium orientation or a unique, globally attracting limit cycle. It is important to note that one need not perform the entire analysis to determine what type of behaviour will occur in a steady flow: if there is a positive real eigenvalue of $\boldsymbol{\kappa}$, then the attractor is a steady orientation; if there is no positive real eigenvalue, the attractor is a limit cycle in a plane. In either case, all particles forget their initial orientation, except that the 'phase' of motion on the limit cycle is a function of initial orientation. We derived appropriate strong flow criteria for stretch of the particles in both cases by analysing stretch of the particles which follow the relevant attractor for the orientation dynamics.

In time-periodic flows, we analysed orientation dynamics in the Poincaré map constructed from the equivalent deformation gradient tensor $\boldsymbol{Q}$. We showed there is either a globally attracting fixed orientation, or a globally attracting invariant great circle. These motions correspond to a periodic integral curve of the underlying differential equation or to a quasi-periodic integral curve, respectively. Thus, the orientation dynamics is phase locked with the forcing, or quasi-periodic. In either case, all initial orientations are forgotten, except that the 'phase' on the quasi-periodic attractor depends on initial orientation. Again, we remark that one need not perform the entire analysis to determine what type of behaviour will occur in a time-periodic flow: if there is a real eigenvalue of $\boldsymbol{Q}$ greater than 1, then the attractor is a phase-locked limit cycle; if there is no real eigenvalue of $\boldsymbol{Q}$ greater than 1, the attractor is quasi-periodic. We derived a strong flow criteria in the phase-locked case.

The complexity of the orientation dynamics in the case of a quasi-periodic attractor motivated the development of weak flow criteria for the stretch of particles in a flow. In the first such criterion, we neglected the details of the history of the orientation dynamics, but retained the history of the flow. In a second criterion, we disregarded the detailed history of the flow as well. These criteria will no doubt find application in flows of a more complicated time-dependent nature than those we could treat analytically.

This work was supported, in part, by grants from the Office of Naval Research, and by the Fluid Mechanics Program of the National Science Foundation. A.S. is grateful to U. F. González for reading the manuscript, and to a particularly helpful referee.

REFERENCES

ARNOL'D, V. I. 1973 *Ordinary Differential Equations*. MIT Press.

BRETHERTON, F. P. 1962 The motion of rigid particles in a shear flow at low Reynolds number. *J. Fluid Mech.* **14**, 284–304.

CULLEN, C. G. 1979 *Linear Algebra and Differential Equations*. Prindle, Weber and Schmidt.

JEFFERY, G. B. 1922 The motion of ellipsoidal particles immersed in a fluid. *Proc. R. Soc. Lond.* A **102**, 161–179.

LIPSCOMB, G. G., DENN, M. M., HUR, D. U. & BOGER, D. V. 1988 The flow of fiber suspensions in complex geometries. *J. Non-Newtonian Fluid Mech.* **26**, 297–325.

OLBRICHT, W. L., RALLISON, J. M. & LEAL, L. G. 1982 Strong flow criterion based on microstructure deformation. *J. Non-Newtonian Fluid Mech.* **10**, 291–318.

SZERI, A. J. 1993 Pattern formation in recirculating flows of suspensions of orientable particles. *Phil. Trans. R. Soc. Lond.*, to appear.

SZERI, A. J., MILLIKEN, W. J. & LEAL, L. G. 1992 Rigid particles suspended in time-dependent flows: irregular versus regular motion, disorder versus order. *J. Fluid Mech.* **237**, 33–56.

SZERI, A. J., WIGGINS, S. W. & LEAL, L. G. 1991 On the dynamics of microstructure in unsteady, spatially inhomogeneous, two-dimensional fluid flows. *J. Fluid Mech.* **228**, 207–241 (referred to herein as SWL).

THOMPSON, J. M. T. & STEWART, H. B. 1986 *Nonlinear Dynamics and Chaos*. J. Wiley & Sons.